

## Coil Evaluation Metrics

Jinfeng Tian<sup>1</sup>, Lance Delabarre<sup>2</sup>, and J. Thomas Vaughan<sup>2</sup>

<sup>1</sup>CMRR - Dept. of Rad., U. of Minnesota, Minneapolis, Minnesota, United States, <sup>2</sup>CMRR - Dept. of Rad., U. of Minnesota, Minnesota, United States

**Purpose:** To demonstrate the importance of homogeneity over 3D VOIs and  $B_1^+$  efficiency normalized by SAR as evaluation metrics in coil comparison.

**Methods:** Four 3T 70 cm i.d. volume coils were simulated with FDTD modeling (XFDTD, Remcom, PA) on a 180 cm, 72 kg male (Duke of the Virtual Family<sup>1</sup>). The High-Pass Birdcage was 50 cm long; the TEM arrays 45 cm. The labeling "1x8 TEM" represents 1 row of 8 decoupled independently driven TEM microstriplines, 2x8 means the length was split into two rows of coils, and 3x8 - three rows of coils (24 total).<sup>2</sup> The coil was simulated centered over the prostate and the heart. The TEM coils were  $B_1^+$  shimmed, and the input amplitude of the elements near the arms was decreased to reduce SAR. Three 7T head coils were simulated. These were a 32 loop coil with two rows of loops in the z-direction, a 16 channel microstripline coil (TEM 2D), and a 30 channel microstripline coil, Figure 3.<sup>3</sup> The resulting  $B_1^+$  maps were normalized to the power absorbed in the torso (similar to global SAR) instead of net input power to the coil.

**Results & Discussion:** There are several metrics used in evaluating coil designs such as net  $B_1^+$ , SAR, efficiency, and field homogeneity. There are subtle yet important aspects to such evaluations exemplified by this data. First, coil  $B_1^+$  efficiencies are often evaluated as peak  $B_1^+$  per input power. But the volume over which the  $B_1^+$  is distributed and the uniformity over the desired FOV can be overlooked by such a metric. The central coronal slices of Figure 1 show that the first coil has the strongest average  $B_1^+$  in the slice. But as is apparent in the coronal view, and summarized by the average  $B_1^+$  for each transverse slice along the z-dimension shown in figure 2, the signal intensity is focused on the central transverse slices and falls off rapidly to the edge of the FOV. Such inhomogeneity in the z-dimension can lead to position dependent variations in efficiency and substantial flip angle variations in long organs such as the spine or blood vessels. Calculating the efficiency over a target 3D volume (40x50 cm) produces a more representative metric. Secondly, efficiency measures are often stated in terms of  $B_1^+$  per input power. This makes sense if the experiments are limited by only peak power. However, the limiting factor for most imaging studies is SAR, not peak power. In Figure 3, instead of normalizing by input power, the figures are normalized by net SAR in the head. When this is done, there is surprising agreement between three rather dissimilar coil structures. The loop array, shown in the first grayed row of Table 1, is quite efficient at producing  $B_1^+$ , but it seems equally efficient at E-field transmission. These three structures would each be able to produce roughly the same  $B_1^+$  when limited by global SAR. When limited by local SAR, as most high-field experiments are, what appears to be the least efficient head coil, becomes the coil that can generate the largest flip angle. Similar disparities are noted with the 3T body coils in Table 1. Therefore, when comparing coil performance, a metric of B-field / SAR efficiency should be included, such as  $SAR_{10g} / (B_1^+)^2$ .<sup>4</sup>

**Conclusion:** When evaluating a coil, the efficiency should be considered over a 3D volume and an additional efficiency relative to SAR should be included.

**References:** 1) Christ, Phys. Med. Biol 55:1767-83. 2) Tian, ISMRM 2013, 2746. 3) Tian, ISMRM 2013, 2758. 4) Snyder et al, MRM 2012;67(4):954-64.

**Acknowledgements:** Support from NIH-NIBIB 2R01 EB006835, NIH-NIBIB 2R01 EB007327, BTRR NIH-P41 RR08079 & P41 EB015894.

Three metrics of coil efficiency

Coil	Mean $B_1^+$ ( $\mu T$ )	SAR norm. Mean $B_1^+$ ( $\mu T$ )	Peak 10 g SAR (W/kg)	SAR 10 g / $(B_1^+)^2$ (W/kg / $\mu T^2$ )
HPBC	0.1297	0.1297	0.0920	5.468
TEM 1x8	0.1148	0.1354	0.0658	3.589
TEM 2x8	0.0850	0.1373	0.0706	3.745
TEM 3x8	0.0354	0.1293	0.1063	6.358
32-loop	0.5171	0.56	0.89	2.84
TEM 2D	0.3070	0.50	0.56	2.24
TEM 3D	0.3232	0.53	0.67	2.39

**Table 1.** Three metrics of coil efficiency are shown. The white rows are for four 3T body coils centered on the heart. The first column is  $B_1^+$  normalized by input power, the second is  $B_1^+$  normalized by global SAR, and the last column represents how much local SAR is generated to achieve the same flip angle. The shaded rows are for 3 7T head coils as shown in Figure 3. Although the first row of each case produces more  $B_1^+$  per input watt, when normalized to global SAR or local SAR, (the important metric for SAR limited studies) other structures become advantageous.

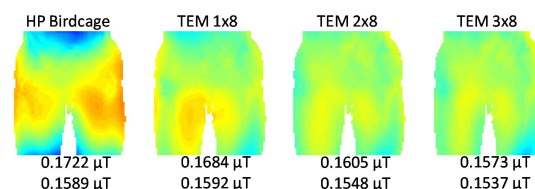


**Fig. 1**  $B_1^+$  of central coronal slices of the pelvis. The figures are normalized to the net power absorbed in the torso. Mean  $B_1^+$  for this 2D slice in  $\mu T$  is displayed in the first row; mean  $B_1^+$  over a large 3D volume in the second row.

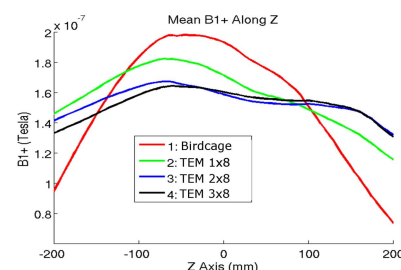


**Fig. 2** For each transverse slice, the average  $B_1^+$  was computed in the VOI.

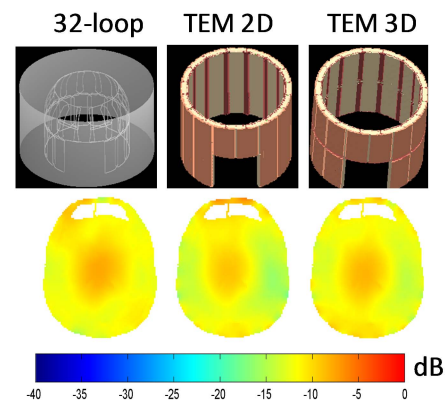


**Fig.3** The  $B_1^+$  of three 7T head coil designs normalized to global SAR.